Journal of Materials Science and Chemical Engineering, 2024, 12, 53-64
https://www.scirp.org/journal/msce
ISSN Online: 2327-6053
ISSN Print: 2327-6045

Effects of Pre-Strain on Bake Hardenability and Precipitation Behavior of Al-Mg-Si Automotive Body Sheets

Guanjun Gao[1,2,3*], Lizhen Yan[1,2,3], Xiwu Li[1,2,3]

[1]State Key Laboratory of Non-Ferrous Metals and Processes, China GRINM Group Co., Ltd., Beijing, China
[2]GRIMAT Engineering Institute Co., Ltd., Beijing, China
[3]General Research Institute for Nonferrous Metals, Beijing, China
Email: *wwwgaoguanjun@126.com

How to cite this paper: Gao, G.J., Yan, L.Z. and Li, X.W. (2024) Effects of Pre-Strain on Bake Hardenability and Precipitation Behavior of Al-Mg-Si Automotive Body Sheets. *Journal of Materials Science and Chemical Engineering*, **12**, 53-64.
https://doi.org/10.4236/msce.2024.127005

Received: June 21, 2024
Accepted: July 28, 2024
Published: July 31, 2024

Abstract

The study investigates the effects of pre-strain on the bake hardenability and precipitation behavior of Al-Mg-Si automotive body sheets. The scanning electron microscopy, transmission electron microscopy, tensile test, Vickers hardness test, and differential scanning calorimetry were conducted for the purpose. It was found that the pre-strain treatment partially inhibits the natural aging hardening effect but cannot completely eliminate it. The pre-straining significantly enhances the bake hardening effect, with the 5% pre-strain sample showing the highest increase in yield strength and hardness. The formation of fine β' precipitates and dislocation structures contribute to the observed strengthening. Additionally, the study highlights the importance of optimizing pre-strain levels to achieve the best balance between strength and ductility in bake-hardened aluminum alloys.

Keywords

Al-Mg-Si Alloy, Pre-Strain, Bake Hardenability, Precipitation Behavior, Clusters

1. Introduction

Compared with traditional steel automotive sheets, Al-Mg-Si alloys are the primary choice of automotive manufacturers to replace steel due to their high strength-to-weight ratio, good formability, and favorable corrosion resistance [1] [2]. To achieve optimal bake-hardening effects, the alloy sheets undergo rapid cooling after solution treatment to obtain a highly supersaturated solid solu-

tion. The sheets have poor deformation resistance at high temperatures, which easily introduces residual stress and may lead to warping. Hence, the stretch-bend straightening process can be employed, causing plastic elongation of the strips below their yield limit to improve the sheet shape.

In industrial production, depending on the degree of warping deformation of the alloy sheets, the deformation amount in stretch-bend straightening generally does not exceed 3%. Extensive research on the pre-strain process of simulated stretch-bend straightening has been conducted both domestically and internationally [3] [4]. The results indicated that the large number of dislocations introduced through deformation can enhance the natural aging hardening effect, while improving the bake-hardening property of alloy sheets. During the stamping process, the alloy sheets can achieve the desired part shape, with an average deformation of approximately 2% and local deformation reaching up to about 15%. After stamping, a large number of dislocations were similarly generated in the matrix, increasing the stored energy within the alloy and providing more nucleation sites for the strengthening phase, thereby enhancing the bake-hardening property of the alloy [5].

During the production process, fine-tuning the alloy composition of aluminum alloy automotive sheets and the deformation amount in stretch-bend straightening have different effects on inhibiting the natural aging hardening effect and improving the bake-hardening property. Therefore, further exploration is needed on the influence of deformation amount in the stretch-bend straightening process on the bake-hardening property and precipitation microstructure of the alloy.

2. Experimental

An Al-Mg-Si ingot with a chemical composition of Al-1.10 wt% Si-0.55 wt% Mg-0.14 wt% Fe-0.10 wt% Cr was fabricated in a resistance furnace. To reduce content segregation, the ingot was first homogenized at 540˚C, then hot rolled, and finally cold rolled to a 1.0-mm-thick sheet. According to the dimensional requirements of the GB/T 228.1 - 2010 standard, tensile samples were taken and processed from the alloy sheet perpendicular to the rolling direction. Tensile samples were directly subjected to solution treatment at 560˚C for 10 min on the ultra-fast solution and quenching heat treatment experimental line, followed by air cooling to room temperature (RT) and immediate immersion in liquid nitrogen to prevent natural aging hardening. The pre-strain treatments were conducted at deformation amounts of 0%, 0.5%, 2%, and 5%. After two weeks of RT storage, the samples underwent T8X treatment (2% deformation + 185˚C for 20 min) and 185˚C for 4 h of bake-hardening treatment. The schematic diagram of the pre-strain treatment process is shown in **Figure 1**.

The mechanical properties and hardness of the alloy samples were measured using an INSTRON 4206 100 kN tensile testing machine and a KB3000BVRZ-SA universal hardness tester. The recrystallized microstructure and fracture surfaces of the alloy were observed and characterized using a QUANTA 600 scanning

electron microscope (SEM) equipped with an electron backscattered diffraction (EBSD) analysis system. After electrolytic dual-jet thinning, microstructure and precipitate phases were observed using a TECNAI G^2 F20 200 kV field emission transmission electron microscope (TEM). Differential scanning calorimetry (DSC) was conducted using a Q100 thermal analyzer to measure the DSC heating curve. Pure aluminum crucibles were used as reference samples, and the process was conducted under argon gas protection during the heating process.

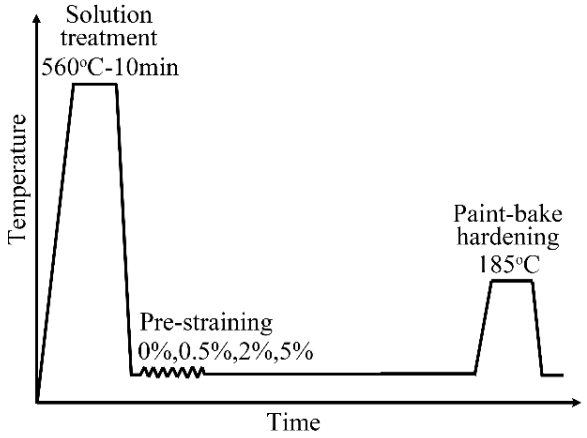

Figure 1. Schematic diagram of pre-strain treatment process for Al-Mg-Si alloy.

3. Results

3.1. Mechanical Properties and Microstructure with Different Strain Levels

Figure 2 shows the stress-strain curves of alloy samples after solution and quenching followed by immediate pre-strain treatments of 0%, 0.5%, 2%, and 5%. The yield strengths of the alloy sheets after deformation were approximately 59.4 MPa, 71.7 MPa, 92.4 MPa, and 133.1 MPa, respectively. It can be seen that

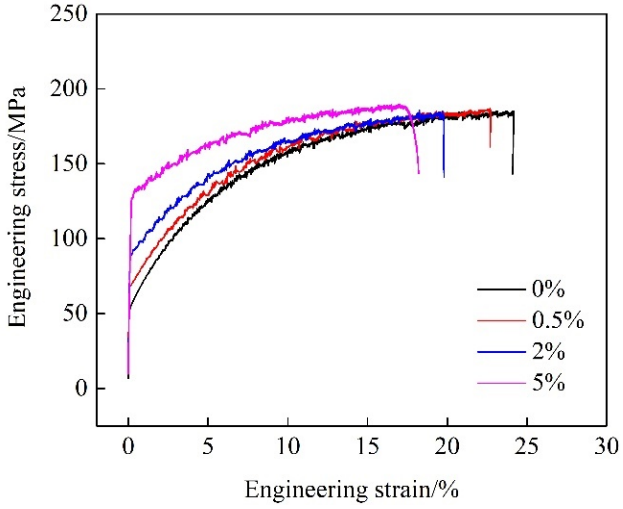

Figure 2. Stress-strain curves of Al-Mg-Si alloy treated with different pre-strain treatments.

with increasing strain levels, the yield strength increased while the fracture elongation decreased. The tensile strengths of the alloy sheets were 185.4 MPa, 187.1 MPa, 185.8 MPa, and 191.6 MPa, respectively, showing minimal variation with strain levels. Compared to conventional curves, the stress-strain curves obtained immediately after solution treatment and pre-strain exhibited serrations rather than smoothness.

After pre-strain treatment, the recrystallized grain morphology of the alloy underwent changes to some extent with increasing strain levels. **Figure 3** shows the microstructure of longitudinal cross-sections of alloy samples after 0%, 0.5%, 2%, and 5% pre-strain treatments. It can be observed that after solution treatment, recrystallization occurred in the alloy sheets, with some recrystallized grains slightly elongated along the rolling direction. According to statistical results, the aspect ratios (length-to-width ratios) of recrystallized grains with different strain conditions are 1.38, 1.30, 1.23, and 1.13, respectively. It was evident that with increasing strain levels, the number of elongated grains decreased, and

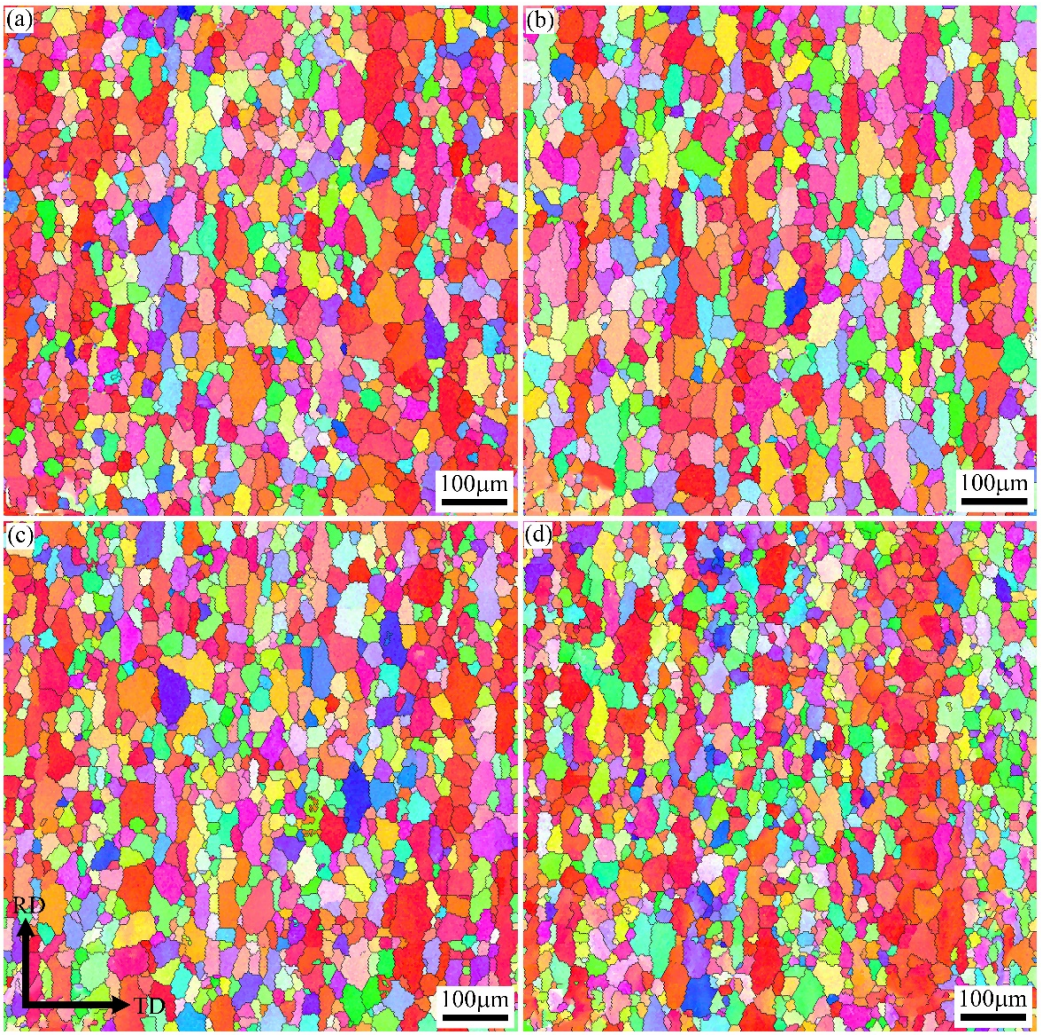

Figure 3. Recrystallization microstructure of alloy samples treated with different pre-strain: (a) 0%; (b) 0.5%; (c) 2%; (d) 5%.

the aspect ratio of recrystallized grains showed a decreasing trend.

Figure 4 shows the fracture surfaces of alloy samples after 0%, 0.5%, 2%, and 5% pre-strain treatments followed by two weeks of RT storage. For the alloy without pre-strain treatment, deep and coarse dimples were present, with a fracture elongation of approximately 25.8%. After 0.5% pre-strain treatment, there were fewer coarse dimples, mainly smaller and shallower ones, with a slight decrease in ductility. At a strain level of 2%, almost no large dimples were observed, and ductility continued to decrease. With a strain level of 5%, the number of small dimples sharply decreased, and in some local areas of the fracture surface, a "river-like" morphology appeared, indicating the absence of dimples, with a fracture elongation decreasing to approximately 19.3%.

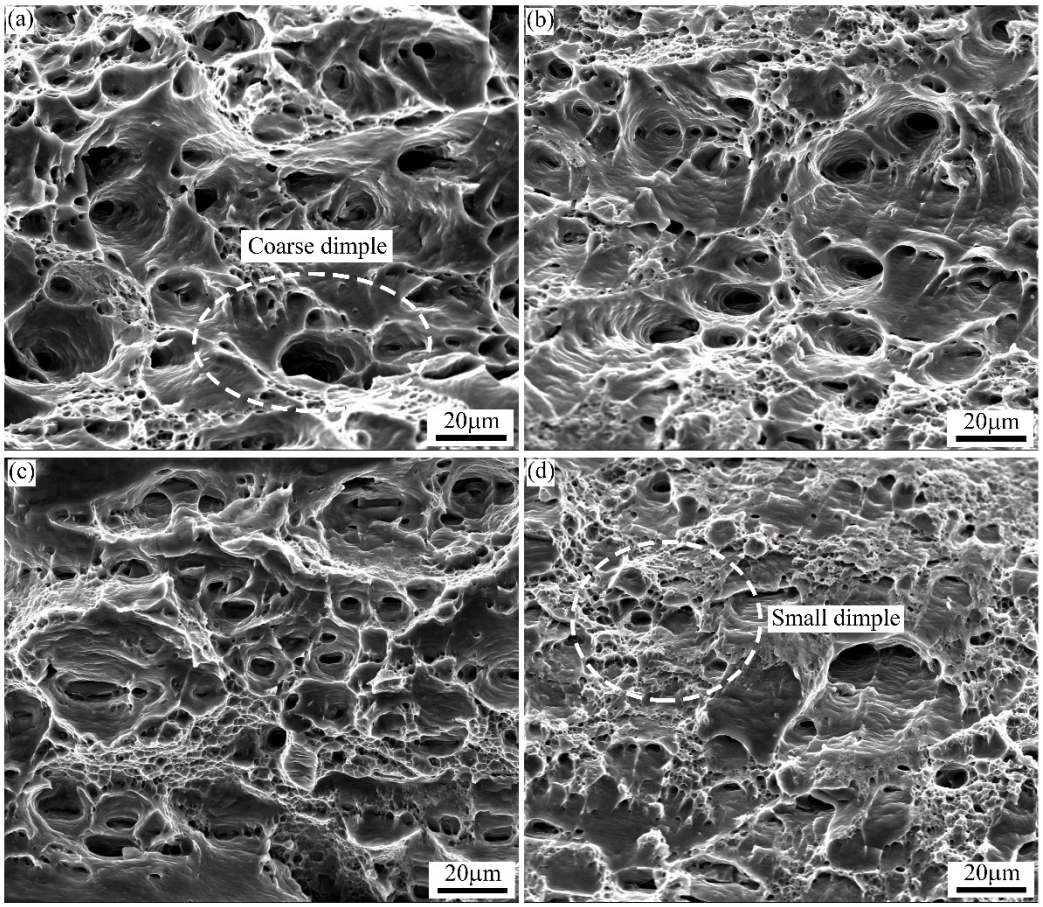

Figure 4. Fracture morphology of alloy samples treated with different pre-strain: (a) 0%; (b) 0.5%; (c) 2%; (d) 5%.

3.2. Changes in Strength during Alloy Room Temperature Storage

After different pre-strain treatments, during the first 12 h of RT storage, significant natural aging strengthening effects were observed in the samples. For the samples without pre-strain, the strength increment was approximately 62.5 MPa, while from 12 h to two weeks of storage, the strength increment was only about 25.4 MPa. The total increase in yield strength of the samples over two weeks of

RT storage was approximately 87.9 MPa. With increasing strain levels, the yield strength increment of the alloy samples gradually decreased. When the strain level was 5%, the yield strength increment of the alloy was about 37.0 MPa. During 12 h to two weeks of storage, the strength increased very slowly, with an increment of only about 11.0 MPa. The total increase in yield strength over two weeks of RT storage decreased to about 48.0 MPa, as shown in **Figure 5**.

3.3. Bake Hardenability and Precipitation Behavior

Figure 6 shows the high resolution transmission electron microscopy (HRTEM) images of alloy samples subjected to 0% and 5% pre-strain treatments followed by two weeks of RT storage. Upon observation, for the alloy sample with 0% strain, numerous atomic clusters of approximately 1 nm in size were present in the matrix. These atomic clusters were fully coherent with the matrix, causing

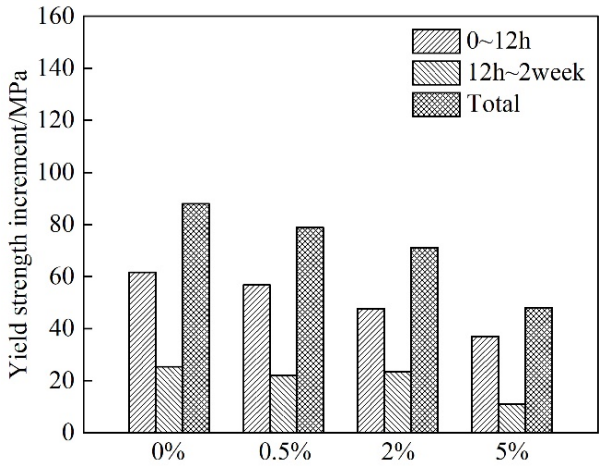

Figure 5. Yield strength increment of alloy samples treated with different pre-strain during RT storage.

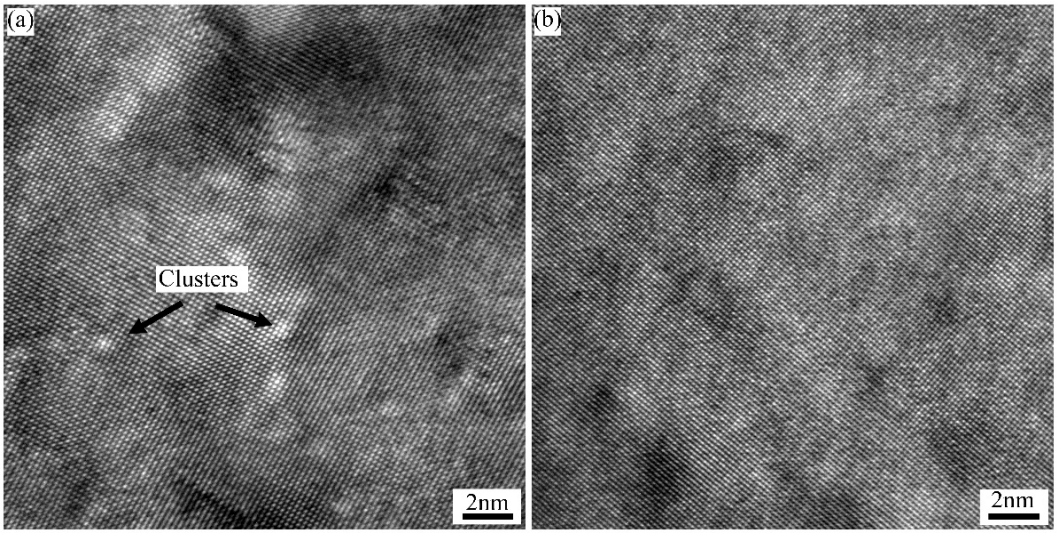

Figure 6. HRTEM images of alloy samples treated with different pre-strain after RT storage for 2 weeks: (a) 0%; (b) 5%.

minor lattice distortions around them. When the strain level was 5%, the number of atomic clusters in the alloy matrix decreased significantly, indicating a reduction in cluster quantity with increasing strain level.

Figure 7 illustrates the yield strength variation of alloy samples after different pre-strain treatments followed by T8X processing. For samples with 0% strain, the yield strength after T8X processing was approximately 161.7 MPa, with a modest increase of about 14.3 MPa in yield strength. With increasing strain levels, the strength after T8X processing significantly increased, and the increment in yield strength also rised accordingly. When the strain level reached 5%, the yield strength after T8X processing was about 220.1 MPa, with an increase in yield strength increment to approximately 39.1 MPa before and after T8X processing.

Figure 8 shows the hardness of alloy samples subjected to different pre-strain treatments and then bake hardening treatment at 185˚C for 4 h. When the deformation amount of the alloy sample was 0%, the hardness after baking treatment reached approximately 109.5 HV. For the alloy sample with a 5% deformation

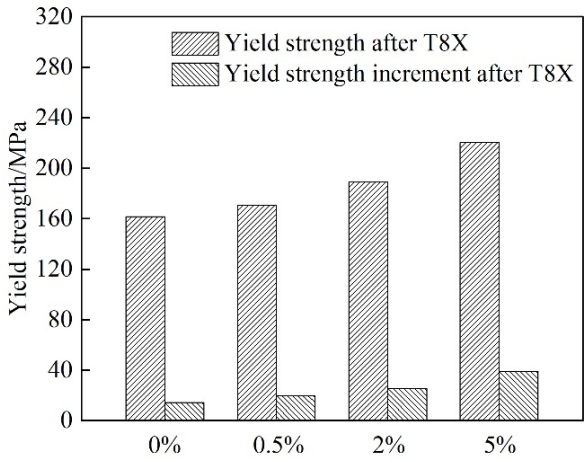

Figure 7. Yield strength of alloy samples treated with different pre-strain after T8X treatment.

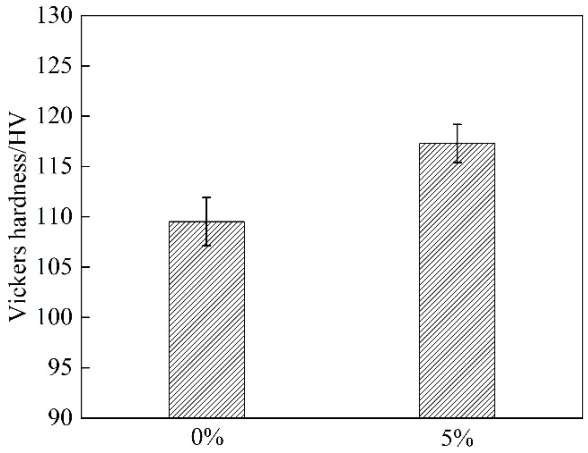

Figure 8. Vickers hardness of alloy samples treated with different pre-strain after 185℃-4 h paint-bake hardening treatment.

amount, the hardness was about 117.3 HV. It was evident that as the deformation amount increased, the Vickers hardness of the alloy samples significantly improved after bake-hardening treatment.

To investigate the effect of pre-strain on bake-hardening, samples with deformation amounts of 0% and 5% were subjected to bake-hardening treatment at 185˚C for 4 h after two weeks of RT storage. The precipitate phases were observed using a TEM, as shown in **Figure 9**. The figure shows that regardless of whether pre-strain treatment was performed, a large number of needle-like β'' strengthening phases formed in the alloy matrix after bake-hardening at 185℃ for 4 h. In the sample with a 5% deformation amount, dislocations formed by pre-strain treatment were also observed. The needle-like β''strengthening phases formed at the dislocations, traversing or pinning them. Furthermore, the β'' strengthening phases in the 5% deformed sample were significantly larger than those in the undeformed sample. In the matrix of the alloy samples, smaller dot-like clusters were also observed, which may have formed during storage at RT. After bake-hardening, these clusters neither dissolved nor transformed and remained in the alloy matrix.

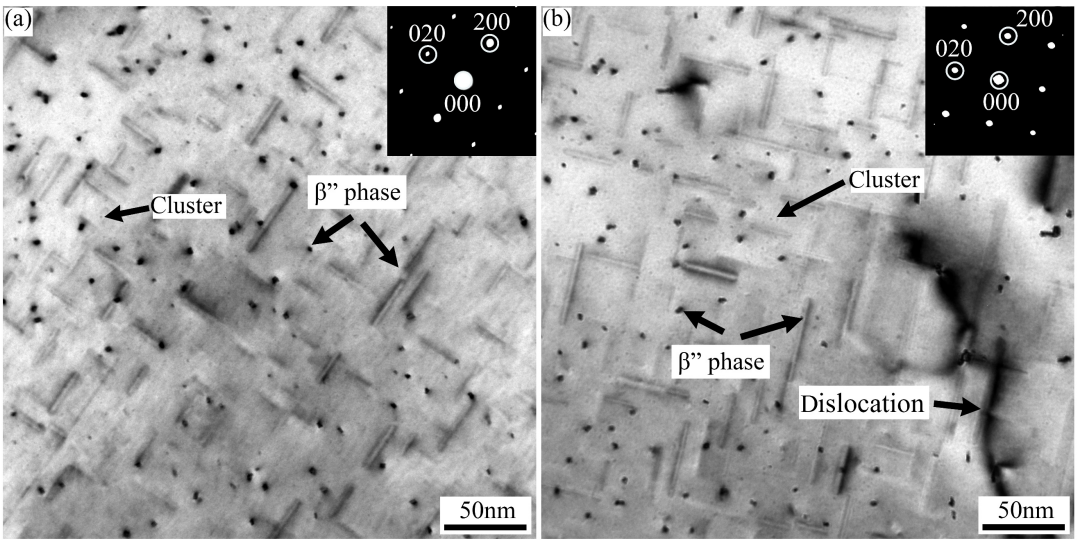

Figure 9. TEM images of alloy samples treated with different pre-strain after 185℃-4 h paint-bake hardening treatment: (a) 0%; (b) 5%.

3.4. Analysis of DSC Curves

Figure 10 shows the DSC heating curves of alloy samples subjected to different pre-strain processes and stored at RT for two weeks. As shown in the figure, there was an endothermic peak and two exothermic peaks on the DSC curves of the alloy samples with different pre-strain amounts. As previously discussed, exothermic peaks II and III corresponded to the precipitation of β'' and β' phases, respectively. With the increase in pre-strain, the temperature corresponding to the exothermic peaks gradually decreased. Specifically, the temperature of the exothermic peak for the β'' phase decreased from 240.1˚C for the non-pre-strained

sample to 233.8˚C for the 5% pre-strained sample.

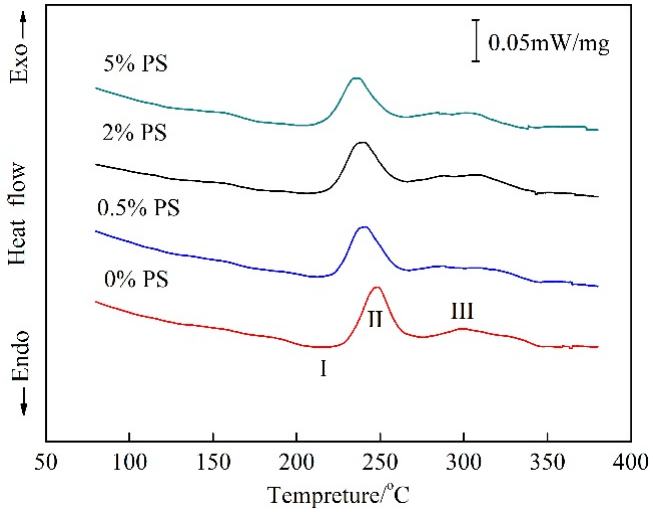

Figure 10. DSC curves of alloy samples treated with different pre-strain after RT storage for 2 weeks

4. Discussion

As the amount of deformation increases, the aspect ratio of the recrystallized grains decreases, but the size change is not significant. Therefore, the influence of grain size on alloy strength is excluded (**Figure 3**). The increase in alloy deformation leads to a rise in dislocation density. Under the influence of stress, a large number of dislocations generated from dislocation sources move along the slip planes, easily intersecting and forming steps, causing dislocation entanglement. These randomly distributed dislocation entanglements can further transform into cellular substructure organizations. The larger the deformation, the finer the substructure, and the stronger the resistance to deformation [6] [7]. Consequently, with the increase in deformation, the alloy strength increases significantly (**Figure 2**). Additionally, from the fracture morphology, it can be seen that with the increase in pre-strain, the alloy transitions from a ductile fracture with significant plastic deformation to a brittle fracture with no significant plastic deformation. This is also due to the increased strength and decreased plasticity of the alloy samples under work hardening (**Figure 4**).

Furthermore, the stress-strain curve obtained from the tensile test immediately after solution treatment and pre-strain processing of the alloy exhibits a serrated yield phenomenon, known as the Portevin-Le Chatelier (PLC) effect (**Figure 2**) [8]. This effect arises from the interaction between mobile dislocations and solute atoms during the plastic deformation of aluminum alloy plates. During deformation, the solute atoms in the aluminum alloy tend to gather around the dislocation lines, forming Cottrell atmospheres. These atmospheres capture the moving dislocations, pinning and locking them, leading to a sudden increase in stress. When the stress reaches a critical value, the dislocations can suddenly break free from the atmospheres, reducing the stress until the moving

dislocations are captured again. This repetitive process results in the appearance of serrations on the stress-strain curve [9].

During the solution treatment and RT storage process of the alloy, if no pre-strain treatment is performed, the supersaturated solute atoms in the matrix rapidly aggregate at RT, forming clusters (1). With the extension of RT storage time, the number of clusters continuously increases, leading to a natural aging hardening effect in the alloy [10]. This hardening effect is particularly evident in the early stages of RT aging, but subsequently weakens due to the consumption of supersaturated solute atoms and vacancies. After solution treatment and pre-strain processing, a large number of dislocations are introduced into the matrix. The formation of these dislocations not only enhances the strength of the alloy but also provides numerous traps for the supersaturated Mg and Si solute atoms and vacancies in the matrix, making solute atom segregation difficult [3]. Although clusters (1) still form during RT storage after pre-strain treatment, their number is significantly reduced, and the increase in yield strength is considerably lower compared to the alloy samples without pre-strain treatment (**Figure 5**). Thus, the pre-strain process can partially inhibit the natural aging hardening effect.

The pre-strain process after solution treatment can not only inhibit the natural aging hardening effect to some extent but also enhance the bake-hardening properties of the alloy sheet. With the increase in pre-strain, both the strength and the increase in strength of the alloy sheet after T8X treatment improve. After 185˚C-4 h bake-hardening treatment, the Vickers hardness of the 5% pre-strained alloy sample is about 7.8 HV higher than that of the unstrained sample (**Figure 8**). Additionally, the DSC curves show that with the increase in pre-strain, the exothermic peak temperature corresponding to the β'' strengthening phase significantly decreases (**Figure 10**). After pre-strain treatment, dislocations are introduced into the matrix, and the energy fluctuations around these dislocations are higher, providing numerous heterogeneous nucleation sites for the precipitated phase during the bake-hardening process [11]. Therefore, pre-strain treatment can promote the formation of the strengthening phase and enhance the bake-hardening properties of the alloy sheet. Moreover, due to the higher strain energy near the dislocations, the precipitated phase can acquire more energy during bake-hardening, resulting in larger β'' phases observed near the dislocations, which are typically distributed in a chain-like continuous or semi-continuous manner [12].

5. Conclusions

In this study, the effects of pre-strain on the bake hardenability and precipitation behavior of Al-Mg-Si automotive body sheets were studied. The following conclusions may be drawn.

1) Pre-strain treatment partially inhibits the natural aging hardening effect but cannot completely eliminate it. The greater the pre-strain, the more significant

the inhibitory effect on natural aging. The yield strength of the unstrained sample increases by approximately 87.9 MPa after two weeks of RT aging, while for a pre-strain of 5%, the increase in yield strength is reduced to about 48.0 MPa.

2) The work hardening induced by pre-strain can damage the formability of the alloy. Therefore, while improving the shape of the sheet, it is essential to minimize the pre-strain in the stretch-bend leveling process.

3) Pre-strain treatment can enhance the bake-hardening properties of alloy sheets. For the sample without pre-strain, the strength increment before and after T8X treatment is only about 14.3 MPa; for the sample with a pre-strain of 5%, the yield strength increment increases to approximately 39.1 MPa. After bake-hardening at 185˚C for 4 h, the hardness of the sample with 5% pre-strain is about 7.8 HV higher than that of the sample without pre-strain.

Acknowledgements

This work was financially supported by the National Key R & D Program of China (2020YFF0218200, No. 2016YFB0300800) and the Innovation Fund Project of GRINM.

Conflicts of Interest

The authors declare no conflicts of interest regarding the publication of this paper.

References

[1] Lu, G., Wang, J., Liu, Y. and Liu, C. (2020) Effect of Heating Rate during Solution Treatment on the Bendability of Al-Mg-Si Alloys. *Materials Science and Engineering*: *A*, **791**, Article ID: 139604. https://doi.org/10.1016/j.msea.2020.139604

[2] Wang, D., Shu, X., Wang, R. and Xu, S. (2020) Mechanism of Necking Defect of 6082 Aluminium Alloy Rolled by Cross-Wedge Rolling Method Based on Material Thermal Properties. *Journal of Central South University*, **27**, 3721-3732. https://doi.org/10.1007/s11771-020-4572-y

[3] Birol, Y. (2005) Pre-Straining to Improve the Bake Hardening Response of a Twin-Roll Cast Al-Mg-Si Alloy. *Scripta Materialia*, **52**, 169-173. https://doi.org/10.1016/j.scriptamat.2004.10.001

[4] Ding, L., Jia, Z., Liu, Y., Weng, Y. and Liu, Q. (2016) The Influence of Cu Addition and Pre-Straining on the Natural Aging and Bake Hardening Response of Al-Mg-Si Alloys. *Journal of Alloys and Compounds*, **688**, 362-367. https://doi.org/10.1016/j.jallcom.2016.07.066

[5] Kwon, Y., Lee, Y.S. and Lee, J.H. (2007) Deformation Behavior of Al-Mg-Si Alloy at the Elevated Temperature. *Journal of Materials Processing Technology*, **187**, 533-536. https://doi.org/10.1016/j.jmatprotec.2006.11.207

[6] Carreño-Morelli, E., Ghilarducci, A.A. and Urreta, S.E. (1999) Dislocation Pinning in a Low-Dose Neutron Irradiated Al-Mg-Si Industrial Alloy. *Philosophical Magazine A*, **79**, 293-304. https://doi.org/10.1080/01418619908210298

[7] Misumi, K., Kaneko, K., Nishiyama, T., Maeda, T., Yamada, K., Ikeda, K., *et al.* (2014) Three-Dimensional Characterization of Interaction between B Precipitate and Dislocation in Al-Mg-Si Alloy. *Journal of Alloys and Compounds*, **600**, 29-33.

https://doi.org/10.1016/j.jallcom.2014.02.059

[8] Cottrell, A.H. (1953) LXXXVI. A Note on the Portevin-Le Chatelier Effect. *The London, Edinburgh, and Dublin Philosophical Magazine and Journal of Science*, **44**, 829-832. https://doi.org/10.1080/14786440808520347

[9] Brindley, B.J. and Worthington, P.J. (1970) Yield-Point Phenomena in Substitutional Alloys. *Metallurgical Reviews*, **15**, 101-114. https://doi.org/10.1179/mtlr.1970.15.1.101

[10] Serizawa, A., Hirosawa, S. and Sato, T. (2008) Three-Dimensional Atom Probe Characterization of Nanoclusters Responsible for Multistep Aging Behavior of an Al-Mg-Si Alloy. *Metallurgical and Materials Transactions A*, **39**, 243-251. https://doi.org/10.1007/s11661-007-9438-5

[11] Wang, Y., Zhao, Y., Xu, X., Pan, D., Jiang, W., Yang, X., *et al.* (2018) Superior Mechanical Properties Induced by the Interaction between Dislocations and Precipitates in the Electro-Pulsing Treated Al-Mg-Si Alloys. *Materials Science and Engineering: A*, **735**, 154-161. https://doi.org/10.1016/j.msea.2018.08.029

[12] Teichmann, K., Marioara, C.D., Andersen, S.J., Pedersen, K.O., Gulbrandsen-Dahl, S., Kolar, M., *et al.* (2011) HRTEM Study of the Effect of Deformation on the Early Precipitation Behaviour in an AA6060 Al-Mg-Si Alloy. *Philosophical Magazine*, **91**, 3744-3754. https://doi.org/10.1080/14786435.2011.593577